crystals

MDPI

Article

Structural Characterization and Molecular Docking Screening of Most Potent 1,2,4-Triazine Sulfonamide Derivatives as Anti-Cancer Agents

Sadaf Mutahir [1,2,*], Muhammad Asim Khan [1,2,*], Ahmed M. Naglah [3,*], Mohamed A. Al-Omar [3], Abdulrahman A. Almehizia [3], Bader Huwaimel [4], Amr S. Abouzied [4,5], Amirah Senaitan Alharbi [6] and Moamen S. Refat [7]

1 School of Chemistry and Chemical Engineering, Linyi University, Linyi 276000, China
2 Department of Chemistry, University of Sialkot, Sialkot 51300, Pakistan
3 Drug Exploration and Development Chair (DEDC), Department of Pharmaceutical Chemistry, College of Pharmacy, King Saud University, P.O. Box 2457, Riyadh 11451, Saudi Arabia
4 Department of Pharmaceutical Chemistry, College of Pharmacy, University of Hail, P.O. Box 2440, Hail 81442, Saudi Arabia
5 Department of Pharmaceutical Chemistry, National Organization for Drug Control and Research (NODCAR), Giza 12553, Egypt
6 King Saud University Medical City, King Khalid University Hospital, P.O. Box 7805, Riyadh 11472, Saudi Arabia
7 Department of Chemistry, College of Science, Taif University, P.O. Box 11099, Taif 21944, Saudi Arabia
* Correspondence: sadafmutahir@hotmail.com (S.M.); khanabdali@hotmail.com (M.A.K.); anaglah@ksu.edu.sa (A.M.N.)

Abstract: One of the biggest problems facing contemporary medicine is cancer. New approaches to therapy are required due to the difficult and prolonged treatment, the numerous adverse properties of the medications employed, and the developing confrontation of neoplastic cells to treatment. Ten 1,2,4-triazine sulfonamide derivatives (**1**–**10**) were chosen for the first time in the current work, and their chemical structures were examined by DFT studies. The in silico flexible docking analysis of the chosen receptors involved in cancer development and metastasis (3RHK, 5GTY, 6PL2, and 7JXH) revealed that the selected compounds are the most promising. The binding affinity of compounds **10**, **2**, **6**, and **4** is much better than the standard drug, Erlotinib, whereas compounds **9**, **3**, **1**, and **7** showed better affinities as compared to standard drugs Neratinib and Tepotinib in the case of 3RHK receptor. The binding affinity against the 5GTY receptor of compounds **10, 5,** and **3** is much better than the standard drug Tepotinib, and compounds **7**, **6**, **2**, **4**, **1**, **8**, and **9** showed better than Erlonitib and Neratinib. The binding affinity against the 6PL2 receptor of compounds **8**, **3**, **5**, **4**, **9**, and **1** is much better than the standard drug Tepotinib. Compounds **10**, **6**, **7**, and **2** were better than Erlotinib and Neratinib. All selected drugs showed better binding affinities than the standard anti-cancer drug Neratinib in the case of the 7JXH receptor, whereas compounds **2**, **10**, **5**, **9**, and **8** are better than Erlotinib. In silico ADME experiments supported the identified compounds' drug similarity. According to the MEP calculations, compounds **3** through **10** can interact non-covalently. The interactions might take the form of σ- and π-hole interactions. Softest compound **4** has the smallest energy gap, with an E-gap value of 3.25 Ev. Compound **4** has the largest energy gap at 3.41 eV. Compound **5** superior electron donor has the highest HOMO energy (6.5470 eV for HOMO). Compound **2** has the lowest LUMO energy, which suggests that it would be the best electron acceptor (E_{LUMO} = 5.766364 eV).

Keywords: 1,2,4-triazine; sulfonamides; anticancer agents; density functional theory; molecular docking; non-covalent interactions; apoptosis

check for updates

Citation: Mutahir, S.; Khan, M.A.; Naglah, A.M.; Al-Omar, M.A.; Almehizia, A.A.; Huwaimel, B.; Abouzied, A.S.; Alharbi, A.S.; Refat, M.S. Structural Characterization and Molecular Docking Screening of Most Potent 1,2,4-Triazine Sulfonamide Derivatives as Anti-Cancer Agents. *Crystals* **2023**, *13*, 767. https://doi.org/10.3390/cryst13050767

Academic Editor: Marian Valko

Received: 15 March 2023
Revised: 20 April 2023
Accepted: 26 April 2023
Published: 4 May 2023

Copyright: © 2023 by the authors. Licensee MDPI, Basel, Switzerland. This article is an open access article distributed under the terms and conditions of the Creative Commons Attribution (CC BY) license (https://creativecommons.org/licenses/by/4.0/).

1. Introduction

Several prescription drugs used in medicine include a heterocyclic core, indicating the importance of this field of chemistry and offering a wide range of opportunities for the creation of novel drugs. Moreover, this field of study has rapidly expanded as a result of novel synthetic methodologies and advanced organic chemistry techniques. The development of anti-cancer drugs is one of the primary goals of heterocyclic chemistry [1]. One of the most commonly used techniques in the development of anti-cancer medications is the synthesis of antimetabolites that structurally resemble naturally occurring critical substrates of metabolic activities. Blocking these vital mechanisms causes cells to proliferate more slowly and go through apoptotic cell death [2]. It is thought that apoptosis is an essential part of how living things function. The immune system's correct growth and operation are its responsibility. Numerous human ailments, such as neurological diseases, autoimmune disorders, and certain cancers, are brought on by the dysregulation of apoptosis. Apoptosis is an active cell death process that is genetically programmed. Apoptotic cells do not cause lysis, inflammation, or harm to nearby cells; they stay whole. One of the main mechanisms of action for many cytotoxic medicines is the stimulation of apoptotic pathways. Furthermore, medication resistance is a common feature of many cancers due to abnormalities in apoptotic signaling. Cytotoxic drugs both stimulate the mitochondrial (intrinsic) and death receptor (extrinsic) apoptosis pathways [3,4].

Nowadays, the majority of anti-cancer medications include proapoptotic qualities. Additionally, the majority of them are made to attain selective activity by utilizing cell division. The selectivity is based on the fact that cancer cells divide more quickly than normal cells. These compounds cause damage to normal cells because they are not adequately selective for cancer cells, which has major ramifications for patients. Therefore, it is crucial to investigate new prospective anti-cancer medicines' cytotoxic and proapoptotic qualities. The movement of phosphatidylserine from a cell's interior side to its outside is one of the distinctive alterations that take place during apoptosis. As a result, it is possible to measure the proapoptotic properties of anti-cancer medications fast and precisely using annexin V, which can form conjugates with a fluorescent dye (FITC). It also makes it possible to utilize flow cytometry to determine when phosphatidylserine is exposed on the cell surface [5].

An important group of molecules with three nitrogen atoms are known as 1,2,4-triazines. These have been discovered to have biological activity and behave similarly to biological substances such as nucleotides or nucleosides. As a result, 1,2,4-triazine derivatives are continually being researched for new uses, one of which is as anticonvulsants for the treatment of epilepsy. At the moment, their attention is on examining how well these substances work to cure or prevent modern ailments such as cancer and diabetes [6,7]. Additionally, it has been established that several biological activities, including the inhibition of kinases, agonism, and antagonism in the central nervous system (CNS) and platelet aggregation, depend on compounds with a 1,2,4-triazine ring. Triazines with sulfonamide groups, however, have not yet received much research attention. Due to problems in their preparation, their numbers are likewise restricted [8]. Nonetheless, several 1,2,4-triazine sulfonamides have been shown to have anti-cancer action. One of them is 2-alkylthio-5-chloro-N-(1,2,4-triazin-3-yl) benzenesulfonamides, which were able to stop the development of cancer cells with IC_{50} values in the micromolar or submicromolar range [9]. On the other hand, sulfonamides are used as chemotherapeutic agents and are known to have a variety of biological roles. Recently, the anti-cancer potential of a vast number of new sulfonamide compounds has been investigated. Strong action has been seen with E7010 and E7070 (indisulam), which are now in phase I and phase II advanced clinical investigations, respectively [10–14].

This study's goal was to clarify a 1,2,4-triazine sulfonamide derivative's unique anticancer properties (Figure 1) [15]. Several reactivity parameters, including the HOMO-LUMO energy gap, electron affinity (A), ionization energy (I), electrophilicity index (E), chemical softness (C), and chemical hardness (C), were taken into consideration and discussed. It also focused on density functional theory (DFT) calculations of target molecules

using Gaussian software. The impact of different substituents on the HOMO-LUMO energy gap values was seen. In silico ADME (absorption, distribution, metabolism, and excretion) profiling—which is essential in the prescreening of pharmaceuticals for clinical stages and comprises the characteristics of drug molecules' absorption, distribution, metabolism, and excretion—was used to identify the best candidate medicine. The findings of the anti-cancer screening revealed that several compounds had good efficacy and were more powerful. Molecular docking calculations were passed out through Schrödinger software to examine the ligand attraction for the active sites of protein enzymes selected from the PDB database. The pharmaceutical sector may be interested in these drugs as well. This study's findings might have a significant impact on the development of anti-cancer drugs to cure malignant diseases in the near future.

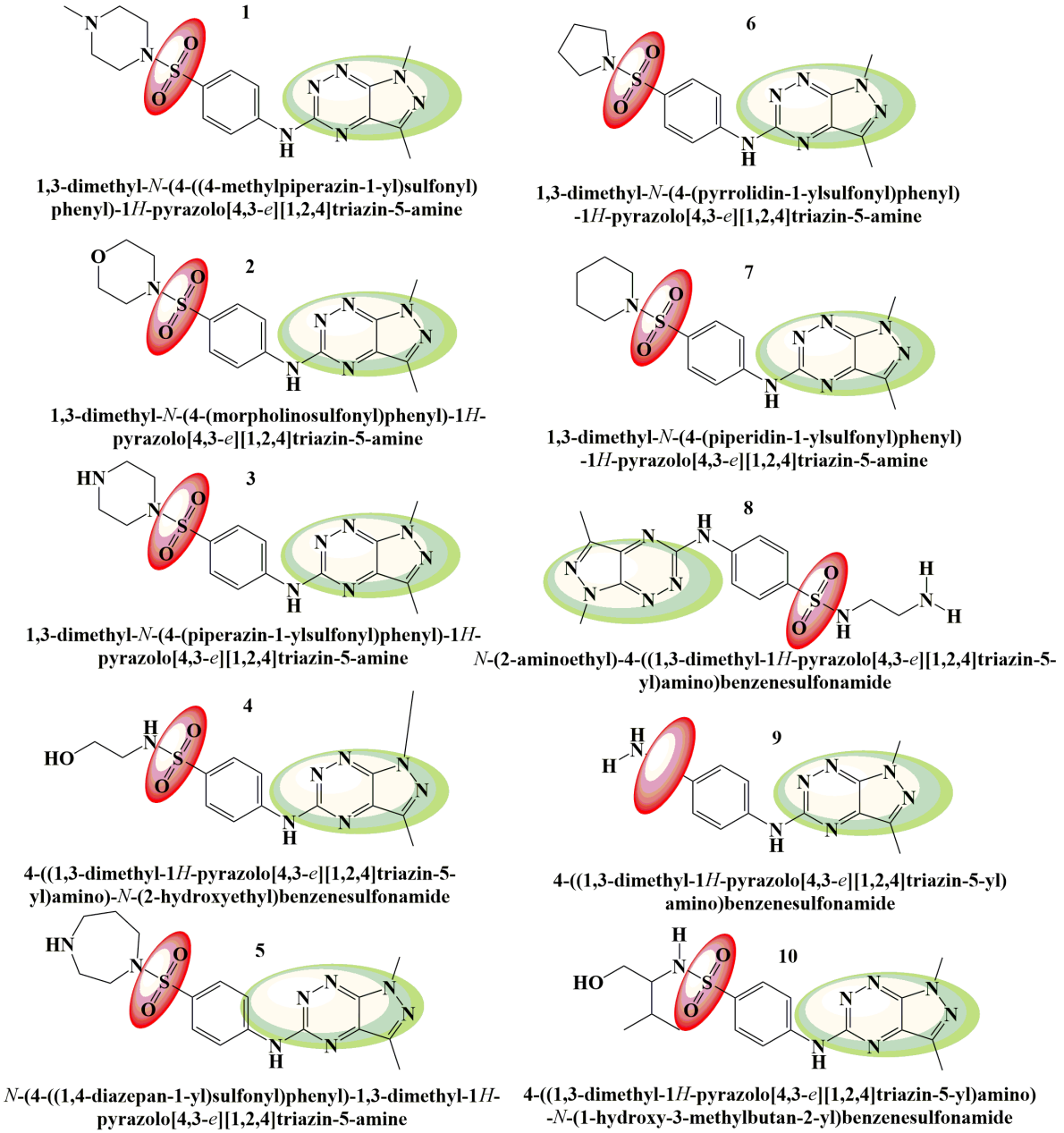


Figure 1. Selected 1,2,4-triazine Sulfonamide Derivatives for the DFT studies and Molecular docking studies as Anti-cancer agents [16].

2. Materials and Methods

2.1. DFT Method

Tools such as Schrödinger and Gaussian have been utilized for molecular docking calculations and density functional theory, respectively. Density functional theory calculations were performed using Gaussian, and a DFT-B3LYP approach and the 6-31G basis set were utilized to optimize the geometry of 1,2,4-triazine sulfonamide derivatives. Analysis of the examined compound's vibrational frequencies, HOMO-LUMO orbitals, and MEP is conducted using the optimized molecular structure. GaussView6 was used to display the results of the HOMO, LUMO, and MEP analyses [17]. Calculations based on theory, the molecular structures, and electronic properties of molecules **1–10** were characterized using theoretical calculations at the DFT/B3LYP/6–31G level for all examined sulfonamides.

2.2. Molecular Docking through Maestro Schrödinger

The structures of 1,2,4-triazine sulfonamide derivatives were optimized using Gaussian, DFT/B3LYP/6–31G level, then imported in Maestro for molecular docking studies to explore changes in the binding mechanism of these compounds and the amino acid sequence of the protein. In addition, their interaction pattern with residues and ligands in the binding site of the protein was determined. Two-dimensional diagrams show the binding poses of these compounds, as well as the binding postures of the interactions of these compounds with protein binding site amino acid residues.

Protein Data Bank PDB Identifiers 3RHK, 5GTY, 6PL2, and 7JXH were used to determine the target protein's structure. Maestro Schrödinger created the protein structure using the Protein Preparation Wizard method; extra chains were removed because just one was needed, and the protein was then reduced and optimized. The protein was passed through the residual process, and finally, a simulation box was created. By locating particular residues that are involved in the target protein's active zone, the grid was built.

After that, the produced ligand and the protein from the grid were put into the Ligand Docking window. Then, the most effective binding method of the active compound within the protein's binding site with the correct orientation was examined [18].

3. Results

3.1. Optimization through Gaussian View

The molecular and electrical structures of the substances under investigation were usefully revealed by theoretical computations. The DFT/B3LYP/6-31G level was theoretically used to determine the electronic properties (Table 1). After energy minimization and shape optimization, compound "**1** to **10**" (Figure 2) was produced [19].

Table 1. Descriptors of global reactivity calculated at the DFT level using basic set /B3LYP/6-311+G level for compounds **1** to **10**.

Ligands	E_{HOMO} (eV)	E_{LUMO} (eV)	ΔE_{gap} (eV)	IE (eV)	A (eV)	μ (eV)	χ (eV)	η (eV)	S (eV)	ω (eV)
1	−5.92	−2.53	3.38	5.92	2.53	−4.22	8.45	1.69	0.295	5.27
2	−5.98	−2.57	3.40	5.98	2.57	−4.27	8.55	1.70	0.293	5.37
3	−5.83	−2.51	3.32	5.83	2.51	−4.17	8.34	1.66	0.300	5.23
4	−6.00	−2.58	3.41	6.00	2.58	−4.29	8.58	1.70	0.292	5.39
5	−5.81	−2.50	3.30	5.81	2.50	−4.16	8.32	1.65	0.302	5.23
6	−5.79	−2.54	3.25	5.79	2.54	−4.17	8.34	1.62	0.307	5.34
7	−5.86	−2.57	3.28	5.86	2.57	−4.21	8.43	1.64	0.304	5.41
8	−5.874	−2.57	3.29	5.87	2.578	−4.22	8.45	1.64	0.303	5.41
9	−5.88	−2.57	3.30	5.88	2.57	−4.23	8.46	1.65	0.302	5.41
10	−5.87	−2.58	3.28	5.87	2.58	−4.22	8.45	1.64	0.304	5.43

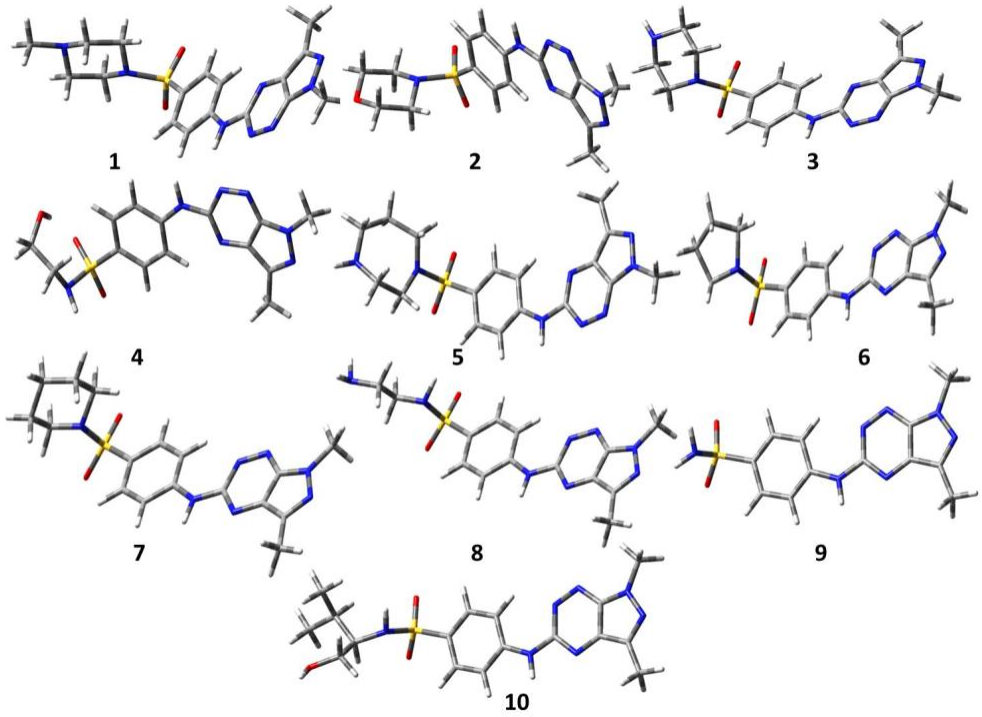


Figure 2. Optimized structures of selected 1,2,4-triazine Sulfonamide Derivatives.

3.2. Descriptors of Global Reactivity

An essential factor in determining the molecule's electronic transport capabilities is the energy gap between the HOMO and LUMO states (Figure 3). Descriptors of a molecule's overall chemical reactivity, such as hardness (η), chemical potential (μ), softness (S), electronegativity (χ), and electrophilicity index (ω), are determined using the HOMO and LUMO energy values for the molecule. The following equation is used to compute them based on the E HOMO and E LUMO—Koopman's theorem application to closed-shell molecules [20].

$$\text{Electrophilicity index } \omega = \mu/2\eta\ 2$$

$$\text{Chemical softness } S = 1/2\eta$$

$$\text{Chemical hardness } \eta = (I - A)/2$$

$$\text{Chemical potential } \mu = -(I + A)/2$$

$I = -E_{HOMO}$ and $A = -ELUMO$ are the orbital energies that may be employed to represent the ionization potential (I) and electron affinity (A). Table 1 displays all of the estimated values for the softness, ionization potential, hardness, electron affinity, potential, and electrophilicity index [20].

Compound **6** has the smallest energy gap, with an ΔE-gap value of 3.250 eV. It is the softest molecule because of the small difference. Compound **1** has the largest energy gap at 3.41 eV, indicating that it is the hardest compound. Compound **4** has the highest HOMO energy at −6.00 eV. Its high energy makes it a superior electron donor. Compound **5** has the lowest LUMO −2.50 eV energy, which suggests that it would be the best electron acceptor. Ionization potential and affinity are crucial properties that must be determined to predict the dynamic stability and chemical reactivity of molecules [21].

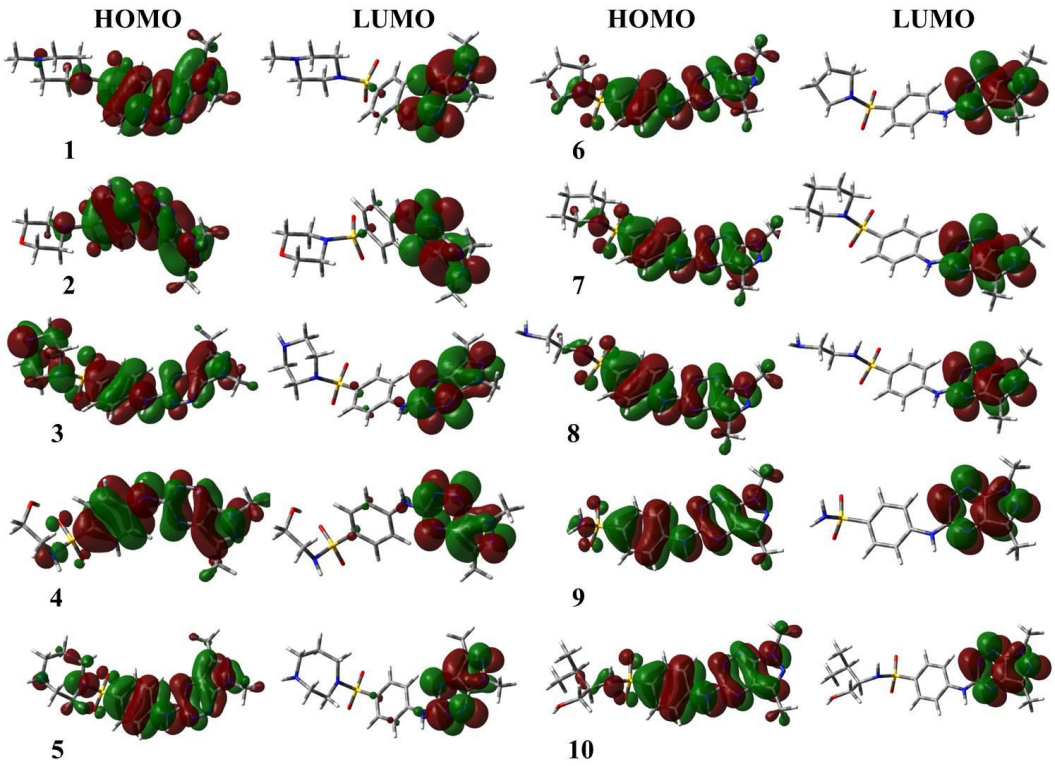


Figure 3. Graphical representation of HOMO and LUMO orbitals of selected 1,2,4-triazine Sulfonamide Derivatives.

3.3. Molecular Electrostatic Potential (MEP) Analysis

The relative reactivity locations of nucleophilic and electrophilic spell sites in a molecule are predicted using MEP. The compound's MEP surface analysis was established utilizing the DFT/B3LYP/6-31G approach with an optimized structure. The molecular electrostatic potential (MEP) can be a useful method for verifying data, indicating that these compounds interact as inhibitors. MEP uses color categorization to define a molecule's size, shape, and positive, negative, and neutral areas. Red, orange, yellow, green, and blue are the colors in ascending order of potential. By following the ring arrangement, it is quite simple to locate places that are suitable for nucleophile and electrophile assault. In contrast to the red color, which represents regions of low electrostatic potential and indicates an abundance of electrons, the blue color denotes the region of extreme electrostatic potential, which designates the nonexistence of electrons in this region and makes it a preferred site for nucleophilic attack. The oxygen atoms of the nitro group (red coded area) in each system are assigned regions of minimal potential following the MEP analysis, as illustrated in the Figure 4. The benzene ring's hydrogen demonstrates that it is a positive compound [22,23].

3.4. Molecular Docking Assay

Molecular docking helps predict inhibition and plays an important role in drug design. It is the main key in the discovery of new medicinal compounds through in silico studies. However, docking facilitates the understanding of the mechanism of action between any ligand and protein, as well as revealing how the ligand interacts with the protein. The docking process can be a single-setup or double-setup calculation. Docking is initiated by selecting the docking parameter. For the ligand docking experiment, the default docking setup settings were used. The binding energies of ligands within the active region of a protein are predicted by a gliding experiment. Maestro was used to obtain 3D and 2D graphics of both best-scoring docking compounds. All ligands gave different values in tabular form with a given protein. This table shows how docking can be effective or not.

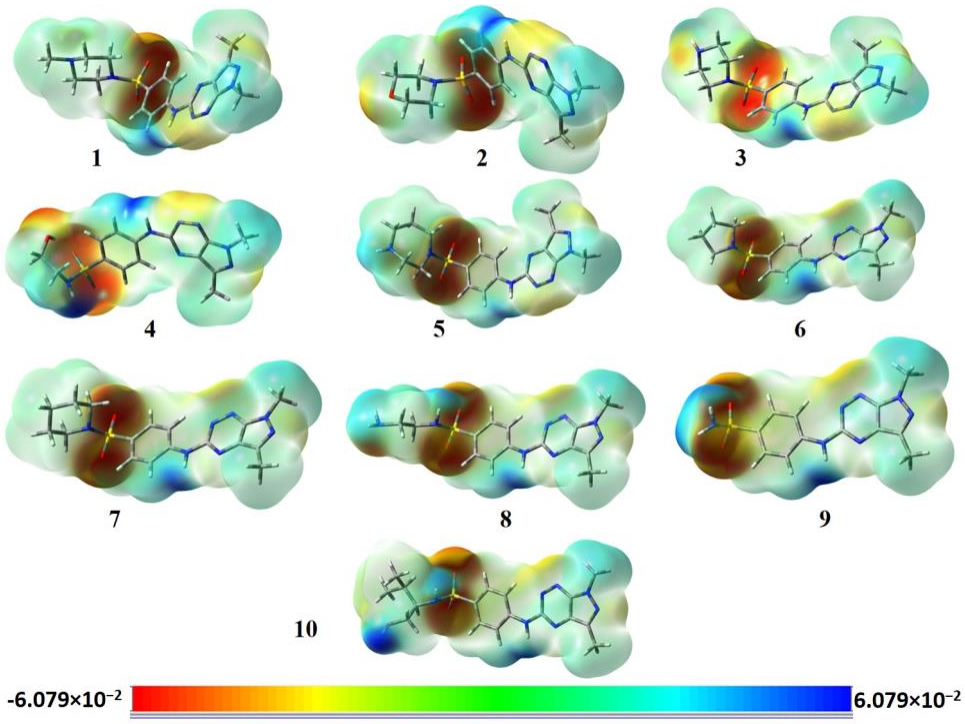


Figure 4. Molecular electrostatic potential (MEP) analysis of selected 1,2,4-triazine Sulfonamide Derivatives.

The reference medications (Erlotinib, Neratinib, and Tepotinib) and selected compounds **1**–**10** were assessed for their ability to bind to the chosen receptors using docking studies cMet, EGFR, HER2, and hTrkA (PDB codes: 3RHK, 5GTY, 7JXH, and 6PL2, respectively) [24–27]. The four selected receptors are widely known for their significance in the development and spread of cancer. Compounds **1**–**10** were docked after the docking protocol had been validated, and their docking scores and ΔG energies were assessed. Their presentation was then equated to the binding similarities of recognized inhibitors of the 3RHK (Figure 5), 5GTY (Figure 6), 6PL2 (Figure 7), and 7JXH (Figure 8) receptors, explicitly Erlotinib, Tepotinib, and Neratinib (Table 2) [28–30]—the chosen compounds whose in vivo studies are reported against anti-cancer agents. According to the reported data in vivo studies, compounds **3** and **5** are highly potent inhibitors, and our in silico results also aligned with the reported data. Among **3** and **5**, compound **3** is potent against all four selected cancer proteins, whereas compound **5** shows potency against 5GTY, 6PL2, and 7JXH. Docking scores/energies are given in Table 2; snapshots of the docked compounds were also produced, which showed the lowest docking scores. The predicted binding interactions for the 3RHK receptor suggested that the docking scores (kcal/mol) were in the range of −2.261 kcal/mol to −5.277 kcal/mol, and ΔG energies were from −22.686 kcal/mol to −37.568 kcal/mol, which represented well to excellent interactions compared to standard drugs. According to the projected binding interactions for the 5GTY receptor, the docking scores (kcal/mol) were between −7.791 and −9.498, and the ΔG energies were between −46.033 and −61.971, which indicated well to exceptional interactions in comparison to conventional medicines. According to the projected binding interactions for the 6PL2 receptor, the docking scores (kcal/mol) were between −2.287 and −5.146, and the ΔG energies were between −27.867 and −39.877, which indicated well to exceptional interactions in comparison to conventional medicines. The docking scores (kcal/mol) were in the range of −5.655 kcal/mol to −6.634 kcal/mol, and ΔG energies were from −44.485 kcal/mol to −51.322 kcal/mol, which revealed that the anticipated binding interactions for the 7JXH receptor constituted good to exceptional interactions relative to typical medicines [31].

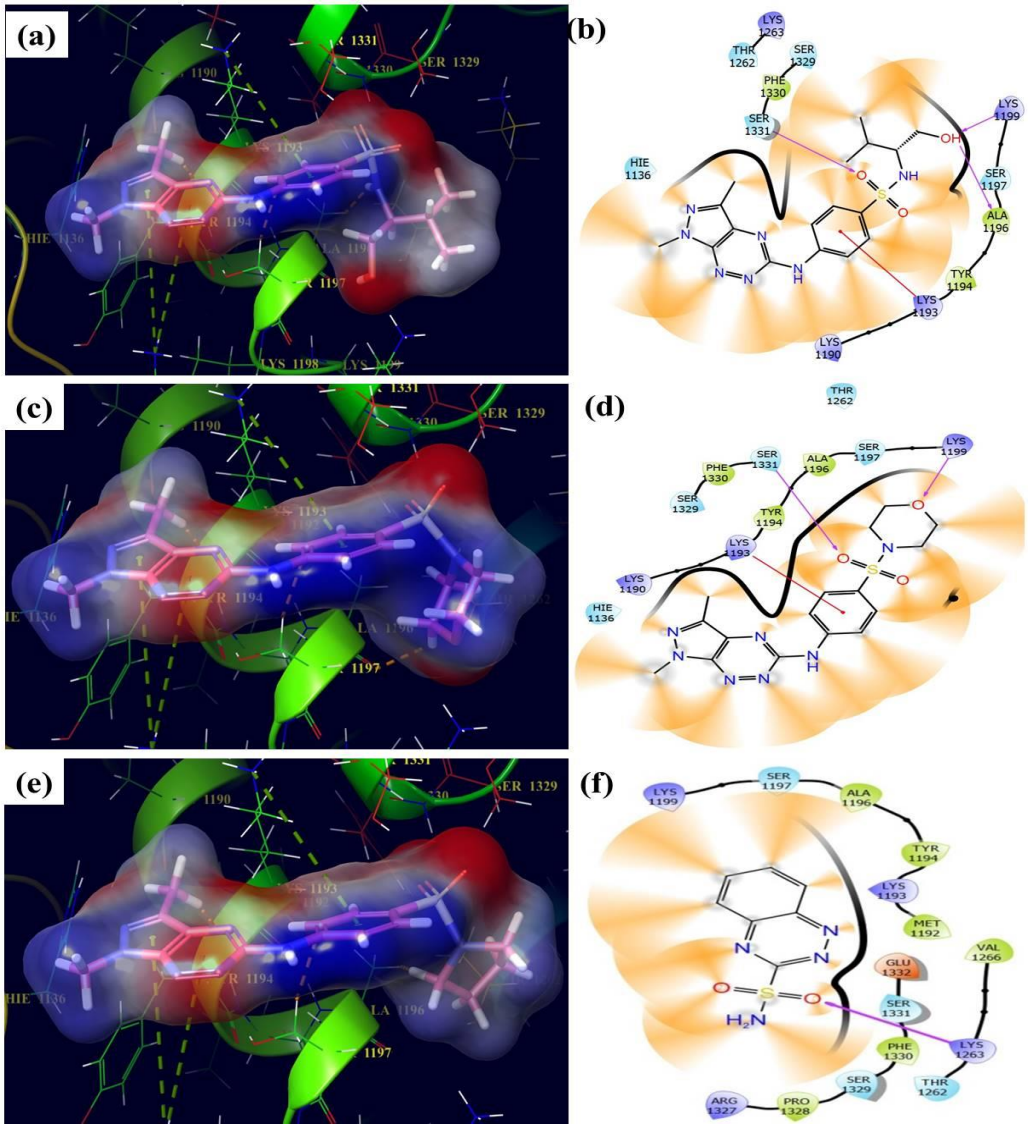


Figure 5. Three-dimensional molecular docking images (**a**,**c**,**e**) and two-dimensional ligand interaction images (**b**,**d**,**f**) of 1,2,4-triazine sulfonamides derivatives (**10** (**a**,**b**), **2** (**c**,**d**), **3** (**e**,**f**), and **3RHK**).

Table 2. The examined ligand-receptor complexes' docking scores and ΔG energy of selected 1,2,4-Triazine Sulfonamide Derivatives (Values are expressed in kcal/mol).

Ligand	3RHK		5GTY		6PL2		7JXH	
	Docking Score kcal/mol	ΔG Energy kcal/mol	Docking Score kcal/mol	ΔG Energy kcal/mol	Docking Score kcal/mol	ΔG Energy kcal/mol	Docking Score kcal/mol	ΔG Energy kcal/mol
1	−3.101	−29.511	−8.204	−50.933	−3.884	−35.62	−5.655	−46.97
2	−4.374	−33.526	−8.572	−52.125	−2.287	−27.867	−6.634	−46.897
3	−3.238	−32.331	−9.03	−56.017	−4.835	−37.531	−6.124	−49.091
4	−4.181	−37.568	−8.449	−53.274	−4.075	−34.647	−6.258	−50.734
5	−2.261	−22.686	−9.099	−56.537	−4.522	−39.877	−6.587	−46.836
6	−4.224	−32.129	−8.608	−52.009	−2.998	−33.2	−6.025	−47.675
7	−3.081	−27.479	−8.727	−54.31	−2.864	−30.155	−6.143	−46.758
8	−2.765	−25	−7.791	−53.477	−5.146	−36.581	−6.462	−50.689
9	−3.963	−32.622	−7.666	−46.033	−3.989	−30.021	−6.491	−44.485
10	−5.277	−37.388	−9.498	−61.971	−3.26	−35.013	−6.617	−51.322

Table 2. *Cont.*

Ligand	3RHK		5GTY		6PL2		7JXH	
	Docking Score kcal/mol	ΔG Energy kcal/mol	Docking Score kcal/mol	ΔG Energy kcal/mol	Docking Score kcal/mol	ΔG Energy kcal/mol	Docking Score kcal/mol	ΔG Energy kcal/mol
Erlotinib	−4.143	−32.362	−7.629	−54.808	−2.279	−31.124	−6.327	−52.283
Neratinib	−2.894	−36.451	−5.674	−58.645	−0.676	−28.228	−4.009	−52.789
Tepotinib	−2.811	−36.912	−9.029	−66.287	−3.339	−47.78	−7.204	−59.378

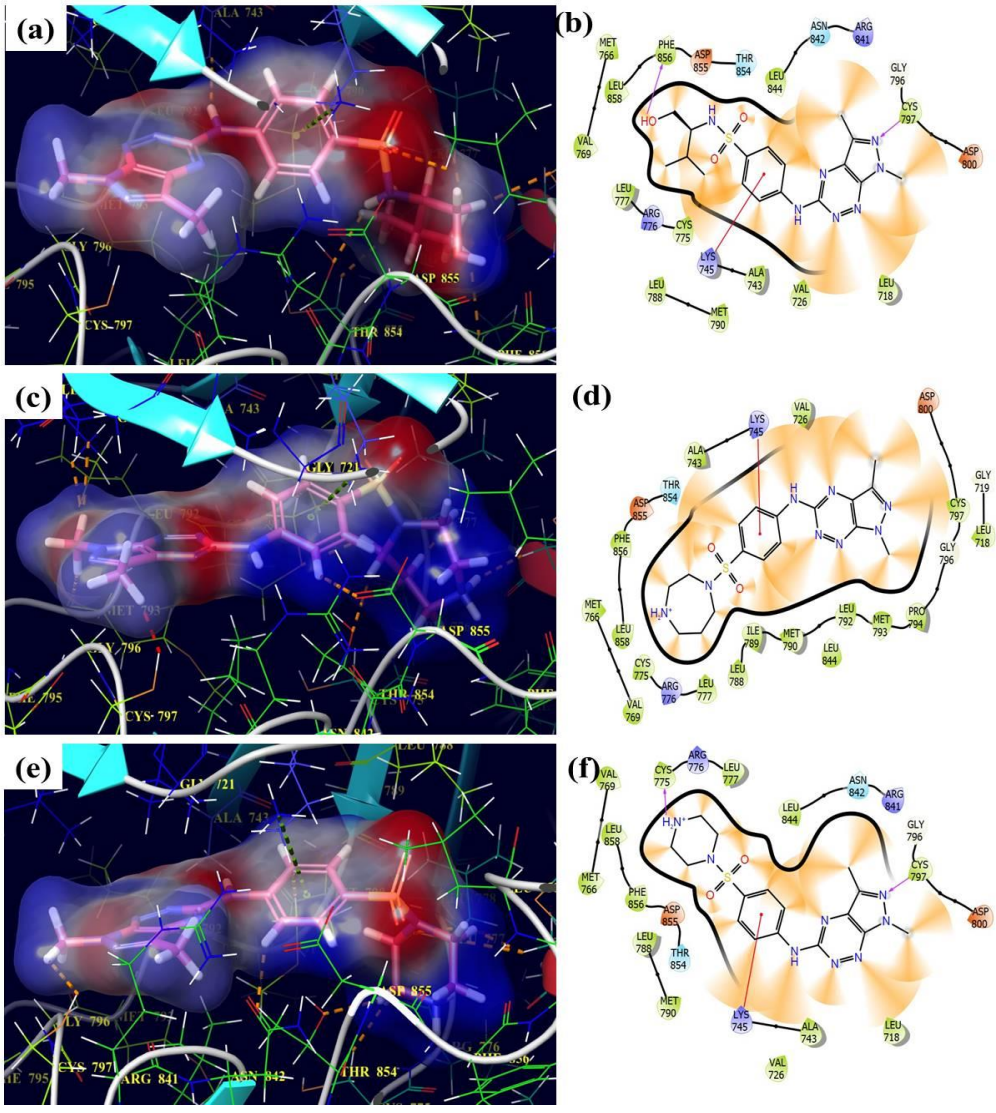


Figure 6. Three-dimensional molecular docking images (**a**,**c**,**e**) and two-dimensional ligand interaction images (**b**,**d**,**f**) of 1,2,4-triazine sulfonamides derivatives (**10** (**a**,**b**), **5** (**c**,**d**), **3** (**e**,**f**), and 5GTY).

When the binding attraction to the selected receptors was analyzed, compounds **10**, **2**, and **3** were the most intriguing ones. Although the ligands **10**, **2**, and **3** have shown the lowest docking scores, these derivatives are inserted well into the binding pockets of the receptor (3RHK). In ligands **10**, **2**, and **3,** the oxygen of the sulfonamides group made a hydrogen bond with the SER-1331 and LYS-1263 residue of the receptor. The binding affinity of compounds **10**, **2**, **6**, and **4** is much better than the standard drug, Erlotinib, whereas compounds **10**, **2**, **6**, **4**, **9**, **3**, **1**, and **7** showed better affinities as compared to standard drugs Neratinib and Tepotinib.

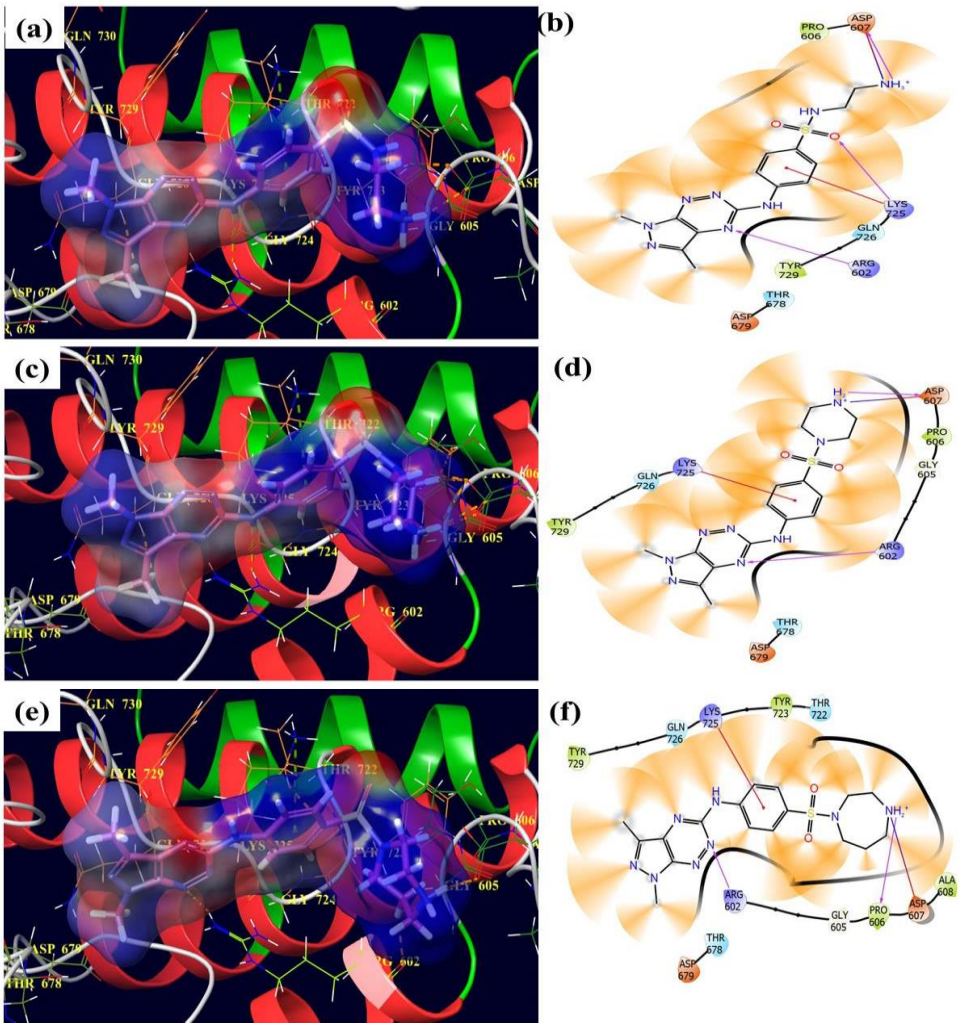


Figure 7. Three-dimensional molecular docking images (**a**,**c**,**e**) and two-dimensional ligand interaction images (**b**,**d**,**f**) of 1,2,4-triazine sulfonamides derivatives (**8** (**a**,**b**), **3** (**c**,**d**), **5** (**e**,**f**), and 6PL2).

The ligands **5**, **6**, and **10** have shown the lowest docking scores; these derivatives were inserted well into the binding pockets of the receptor (5GTY). The structure of ligand **10** is more flexible and showed a stronger affinity with the receptor (PHE-856), whereas, in ligand **5,** the phenyl ring (LYS-745), and in ligand **3,** the nitrogen of an amino group made a hydrogen bond with (CYS-775) residue of the receptor. The binding affinity of compounds **10**, **5**, and **3** is much better than the standard drug Tepotinib, and compounds **7**, **6**, **2**, **4**, **1**, **8**, and **9** showed better than Erlotinib and Neratinib.

The receptor's biding pockets were well inserted by the ligand derivatives **8**, **3**, and **5**, which had the lowest docking scores (6PL2). In ligand **8,** the 1,2,4-triazine rings made a hydrogen bond with the receptor residue LYS-725 and ARG-602. In ligand **3**, the nitrogen of the 1,2,4-triazine ring-shaped formed a hydrogen bond with the receptor residue ARG-602, and in ligand **5,** the sulfonamide nitrogen and oxygen formed a hydrogen bond with the receptor residues LYS-725 and PRO-606. The binding affinity of compounds **8**, **3**, **5**, **4**, **9**, and **1** is much better than the standard drug Tepotinib. Compounds **10**, **6**, **7**, and **2** were better than Erlotinib and Neratinib.

The ligands **2**, **10**, and **5** have shown the lowest docking scores; these derivatives were inserted well into the binding pockets of the receptor (7JXH). In ligands **2**, **10**, and **5**, the 1,2,4-triazine ring made π- π bond with PHE-864 residue of the receptor, whereas in ligand **10,** the nitrogen of 1,2,4-triazine ring and ring itself made π- π bond with ASP-863 and LYS-753 residues of the receptor, respectively, and in ligand **9,** the nitrogen of amino group

and nitrogen of sulfonamide group made a hydrogen bond with SER-783 and ASP-863 residues of the receptor respectively. All selected drugs showed better binding affinities than the standard anti-cancer drug Neratinib in the case of the 7JXH receptor [32].

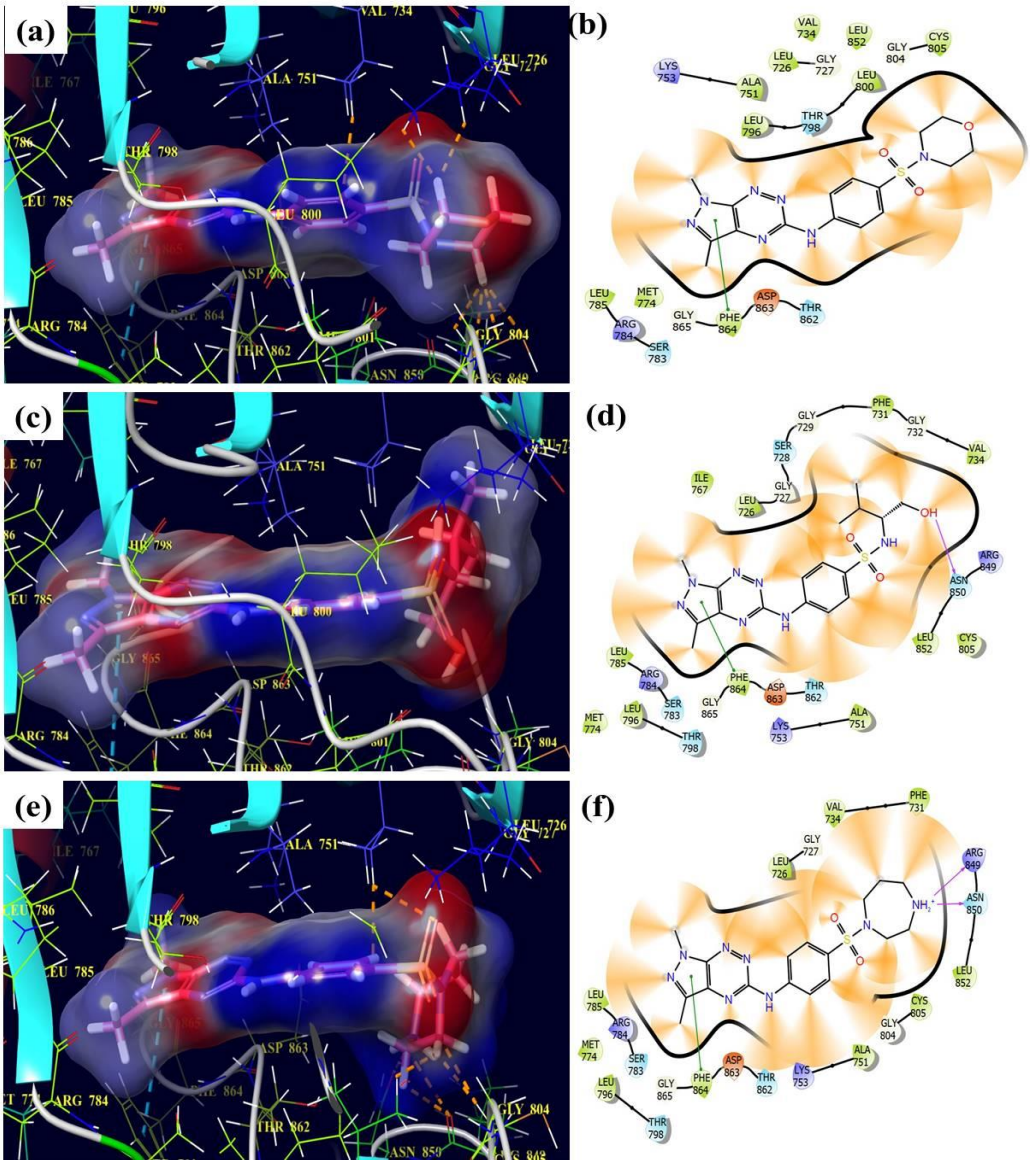


Figure 8. Three-dimensional molecular docking images (**a**,**c**,**e**) and two-dimensional ligand interaction images (**b**,**d**,**f**) of 1,2,4-triazine sulfonamides derivatives (**2** (**a**,**b**), **10** (**c**,**d**), **5** (**e**,**f**), and 7JXH).

3.5. Results of ADME

Physicochemical parameters such as molecular weight, dipole moment, volume, polar surface area, solvent accessible surface, brain/blood partition coefficient, human oral absorption, human oral absorption percentage, MDCK cell permeability, rule of five, and rule of three of the twelve molecules, were calculated as part of the ADME study using the Maestro software [33]. Table 3 lists the outcomes of these calculations. Among all the estimated parameters, the rule of three and the rule of five are the two most crucial parameters. For the rule of three, these parameters must have a numerical value ranging from 0 to 3, and 0 to 4 in the rule of five [34]. All compounds were evaluated for their drug-likeness using Lipinski's rule of five, which takes into account their molecular weights (MW), lipophilicity (log P), number of hydrogen bond acceptors (HBA), and number of hydrogen bond donors (HBD). Ten compounds showed no breaches of Lipinski's rule. It

is also said that substances are more likely to be ingested if they meet Jorgensen's rule of three (QPlogS > −5.7, QPPCaco > 22 nm/s, and # Primary Metabolites < 7) with fewer infractions. Jorgensen's rule of three was found to be followed by all compounds. The solubility and permeability of the medication, as well as interactions of the drug with transporters and metabolic enzymes in the gut wall, all have a role in absorption. The majority of the substances demonstrated high values for projected qualitative human oral absorption and 100% for expected human oral absorption.

Table 3. In silico ADME possessions of selected molecules.

Compd	Mol MW	HBD	HBA	QPlog Po/w	QPlogS	QPPCaco	metab	QPlog Khsa	Human Oral Absorption	Percent Human Oral Absorption	Rule of Five	Rule of Three
1	402.473	1	11	1.051	−3.145	87.847	2	−0.387	3	67.89	0	0
2	389.431	1	10.7	1.205	−3.703	366.53	2	−0.529	3	79.892	0	0
3	388.446	2	10.5	0.653	−3.1	42.575	1	−0.336	2	59.928	0	0
4	363.393	3	10.7	0.242	−3.397	60.53	2	−0.639	3	60.254	0	0
5	402.473	2	10.5	0.754	−2.831	48.159	1	−0.288	3	61.479	0	0
6	373.432	1	9	1.745	−4.325	280.231	1	−0.221	3	80.971	0	0
7	387.459	1	9	2.138	−4.774	329.24	1	−0.081	3	84.525	0	0
8	362.409	4	10	−0.052	−2.073	25.439	3	−0.541	2	51.799	0	0
9	319.34	3	9	0.068	−3.242	60.275	1	−0.543	2	59.203	0	0
10	405.474	3	10.7	1.249	−4.018	119.707	2	−0.375	3	71.454	0	0

Descriptor Range or recommended values (according to the QikProp user manual): Molecular weight (130.0–725.0), HBD (0.0–6.0), HBA (2.0–20.0), QPlogPo/w predicted octanol/water partition coefficient (–2.0–6.5). QPPCaco (<25 poor, >500 great), metab (1–8), QPlogKhsa (−1.5–1.5), Percent Human Oral Absorption (>80% is high, <25% is poor), Human Oral Absorption (1, 2, or 3 for low, medium, or high.), Rule of five (0–4), and Rule of three (0–3).

It is noteworthy that drug binding to plasma significantly reduces the amount of the drug in the blood circulation; hence, the less bound a medication is, the better its ability to disperse or cross cell membranes is. Almost all compounds are discovered in the required QPlogKhsa range of −1.5 to 1.5 (prediction of binding to human serum albumin). This indicates that the majority of the compounds are probably free to circulate inside the bloodstream and hence reach the target region. The results of ADME demonstrated that practically all medications contain characteristics of other drugs.

4. Conclusions

1,2,4-triazine sulfonamide derivatives (**1**–**10**) were selected for their virtual screening and DFT calculations to evaluate cancer inhibition potential, and results were compared against standard (Erlotinib, Neratinib, and Tepotinib) anti-cancer drugs. The in silico flexible docking analysis of the chosen receptors involved in cancer development and metastasis (3RHK, 5GTY, 6PL2, and 7JXH) revealed that the selected compounds are the most promising. The binding affinity of compounds **10**, **2**, **6**, and **4** is much better than the standard drug, Erlotinib, whereas compounds **9**, **3**, **1**, and **7** showed better affinities as compared to standard drugs Neratinib and Tepotinib in the case of the 3RHK receptor. The binding affinity against the 5GTY receptor of compounds **10**, **5**, and **3** is much better than the standard drug Tepotinib, and compounds **7**, **6**, **2**, **4**, **1**, **8**, and **9** showed better than Erlonitib and Neratinib. The binding affinity against the 6PL2 receptor of compounds **8**, **3**, **5**, **4**, **9**, and **1** is much better than the standard drug Tepotinib. Compounds **10**, **6**, **7**, and **2** were better than Erlotinib and Neratinib. All selected drugs showed better binding affinities than the standard anti-cancer drug Neratinib in the case of the 7JXH receptor, whereas compounds **2**, **10**, **5**, **9**, and **8** are better than Erlotinib. In silico ADME experiments supported the identified compounds' drug similarity. Chemicals **1** through **10** are capable of non-covalent interaction, according to the MEP calculations. Potential interactions include σ- and π-hole interactions. With an E-gap value of 3.25 Ev, the softest compound **6** has the smallest energy gap. The biggest energy gap, 3.41 eV, is found in compound **1**. HOMO energy is higher in compound **4**, a superior electron donor (−6.00 eV for HOMO). Since compound **5** has the lowest LUMO energy (ELUMO = −2.50 eV), it could be the best

electron acceptor. The results suggest that the selected 1,2,4-triazine sulfonamide motifs have excellent to good potential to be adopted as future anti-cancer drugs.

Author Contributions: Conceptualization, S.M.; methodology, M.A.K.; software, A.M.N., M.A.A.-O. and A.A.A.; validation, B.H. and A.S.A. (Amr S. Abouziedand); formal analysis, A.S.A. (Amirah Senaitan Alharbi) and M.S.R.; investigation, S.M.; resources, S.M. and A.M.N.; writing—original draft preparation, S.M. and M.A.K.; writing—review and editing, A.M.N.; visualization, M.S.R.; supervision, S.M. and M.A.K.; project administration, S.M. and M.A.K. All authors have read and agreed to the published version of the manuscript.

Funding: This research was funded by the Deanship of Scientific Research at King Saud University through the Vice Deanship of Scientific Research Chairs.

Data Availability Statement: Not available.

Acknowledgments: The authors extend their appreciation to the Deanship of Scientific Research, King Saud University, for funding through the Vice Deanship of Scientific Research Chairs; (Drug Exploration and Development Chair).

Conflicts of Interest: The authors declare no conflict of interest.

References

1. Kciuk, M.; Mujwar, S.; Szymanowska, A.; Marciniak, B.; Bukowski, K.; Mojzych, M.; Kontek, R. Preparation of Novel Pyrazolo [4, 3-e] tetrazolo [1, 5-b][1, 2, 4] triazine Sulfonamides and Their Experimental and Computational Biological Studies. *Int. J. Mol. Sci.* **2022**, *23*, 5892. [CrossRef]
2. Villa, E.; Ali, E.S.; Sahu, U.; Ben-Sahra, I. Cancer cells tune the signaling pathways to empower de novo synthesis of nucleotides. *Cancers* **2019**, *11*, 688. [CrossRef] [PubMed]
3. Thomas, E.; Stewart, L.E.; Darley, B.A.; Pham, A.M.; Esteban, I.; Panda, S.S. Plant-Based Natural Products and Extracts: Potential Source to Develop New Antiviral Drug Candidates. *Molecules* **2021**, *26*, 6197. [CrossRef]
4. Hong, P.; Liu, Q.-W.; Xie, Y.; Zhang, Q.-H.; Liao, L.; He, Q.-Y.; Li, B.; Xu, W.W. Echinatin suppresses esophageal cancer tumor growth and invasion through inducing AKT/mTOR-dependent autophagy and apoptosis. *Cell Death Dis.* **2020**, *11*, 524. [CrossRef]
5. Kumar, R.; Saneja, A.; Panda, A.K. An Annexin V-FITC—Propidium Iodide-Based Method for Detecting Apoptosis in a Non-Small Cell Lung Cancer Cell Line. In *Lung Cancer*; Springer: Berlin/Heidelberg, Germany, 2021; pp. 213–223.
6. Shamim, S.; Khan, K.M.; Ullah, N.; Chigurupati, S.; Wadood, A.; Rehman, A.U.; Ali, M.; Salar, U.; Alhowail, A.; Taha, M. Synthesis and screening of (E)-3-(2-benzylidenehydrazinyl)-5, 6-diphenyl-1, 2, 4-triazine analogs as novel dual inhibitors of α-amylase and α-glucosidase. *Bioorganic Chem.* **2020**, *101*, 103979. [CrossRef]
7. Hermanowicz, J.M.; Szymanowska, A.; Sieklucka, B.; Czarnomysy, R.; Pawlak, K.; Bielawska, A.; Bielawski, K.; Kalafut, J.; Przybyszewska, A.; Surazynski, A. Exploration of novel heterofused 1, 2, 4-triazine derivative in colorectal cancer. *J. Enzym. Inhib. Med. Chem.* **2021**, *36*, 535–548. [CrossRef] [PubMed]
8. Lindsley, C.; Layton, M. *Science of Synthesis: Houben-Weyl Methods of Molecular Transformations*; Weinreb, S.M., Ed.; Thieme: New York, NY, USA, 2004; Volume 17, p. 357.
9. Khatir, Z.Z.; Irannejad, H. Pharmacologic Activities of 5, 6-Diaryl/heteroaryl-3-substituted-1, 2, 4-triazines as a Privileged Scaffold in Drug Development. *Mini Rev. Med. Chem.* **2021**, *21*, 2874–2928. [CrossRef] [PubMed]
10. Okolotowicz, K.J.; Dwyer, M.; Ryan, D.; Cheng, J.; Cashman, E.A.; Moore, S.; Mercola, M.; Cashman, J.R. Novel tertiary sulfonamides as potent anti-cancer agents. *Bioorganic Med. Chem.* **2018**, *26*, 4441–4451. [CrossRef] [PubMed]
11. Supuran, C.T. Indisulam: An anticancer sulfonamide in clinical development. *Expert Opin. Investig. Drugs* **2003**, *12*, 283–287. [CrossRef] [PubMed]
12. Ghorab, M.M.; Ragab, F.A.; Heiba, H.I.; Elsayed, M.S.; Ghorab, W.M. Design, synthesis and molecular modeling study of certain 4-Methylbenzenesulfonamides with CDK2 inhibitory activity as anticancer and radio-sensitizing agents. *Bioorganic Chem.* **2018**, *80*, 276–287. [CrossRef] [PubMed]
13. Said, M.A.; Eldehna, W.M.; Nocentini, A.; Fahim, S.H.; Bonardi, A.; Elgazar, A.A.; Kryštof, V.; Soliman, D.H.; Abdel-Aziz, H.A.; Gratteri, P. Sulfonamide-based ring-fused analogues for CAN508 as novel carbonic anhydrase inhibitors endowed with antitumor activity: Design, synthesis, and in vitro biological evaluation. *Eur. J. Med. Chem.* **2020**, *189*, 112019. [CrossRef]
14. Manasa, K.L. E7010: Investigational anticancer agents targeting the microtubules. *Int. J. Pharm. Sci. Res.* **2015**, *6*, 3713.
15. Gornowicz, A.; Szymanowska, A.; Mojzych, M.; Czarnomysy, R.; Bielawski, K.; Bielawska, A. The Anticancer Action of a Novel 1, 2, 4-Triazine Sulfonamide Derivative in Colon Cancer Cells. *Molecules* **2021**, *26*, 2045. [CrossRef]
16. Mojzych, M.; Šubertová, V.; Bielawska, A.; Bielawski, K.; Bazgier, V.; Berka, K.; Gucký, T.; Fornal, E.; Kryštof, V. Synthesis and kinase inhibitory activity of new sulfonamide derivatives of pyrazolo [4, 3-e][1, 2, 4] triazines. *Eur. J. Med. Chem.* **2014**, *78*, 217–224. [CrossRef]

17. Evecen, M.; Çelik, F.; Bektaş, E.; Güler, H.İ.; Ünver, Y. Experimental and theoretical investigations, enzyme inhibition activity and docking study of 5-methyl-4-(2-(piperazin-1-yl) ethyl)-2, 4-dihydro-3H-1, 2, 4-triazol-3-one. *J. Mol. Struct.* **2023**, *1275*, 134679. [CrossRef]
18. Wang, P.; Yan, F.; Dong, J.; Wang, S.; Shi, Y.; Zhu, M.; Ma, H.; Xue, R.; Zhai, D.; Song, X. A Multiple-step Screening Protocol to Identify Norepinephrine and Dopamine Reuptake Inhibitors for Depression. *Phys. Chem. Chem. Phys.* **2023**, *25*, 8341–8354. [CrossRef]
19. Shaker, S.; Gardouh, A.R.; Ghorab, M.M. Factors affecting liposomes particle size prepared by ethanol injection method. *Res. Pharm. Sci.* **2017**, *12*, 346. [CrossRef]
20. Mughal, E.U.; Ashraf, J.; Hussein, E.M.; Nazir, Y.; Alwuthaynani, A.S.; Naeem, N.; Sadiq, A.; Alsantali, R.I.; Ahmed, S.A. Design, Synthesis, and Structural Characterization of Thioflavones and Thioflavonols as Potential Tyrosinase Inhibitors: In Vitro and In Silico Studies. *ACS Omega* **2022**, *7*, 17444–17461. [CrossRef] [PubMed]
21. Sikandar, S.; Zahoor, A.F.; Ghaffar, A.; Anjum, M.N.; Noreen, R.; Irfan, A.; Munir, B.; Kotwica-Mojzych, K.; Mojzych, M. Unveiling the Chemistry and Synthetic Potential of Catalytic Cycloaddition Reaction of Allenes: A Review. *Molecules* **2023**, *28*, 704. [CrossRef]
22. Kohn, W.; Sham, L.J. Self-consistent equations including exchange and correlation effects. *Phys. Rev.* **1965**, *140*, A1133. [CrossRef]
23. Haoyu, S.Y.; He, X.; Li, S.L.; Truhlar, D.G. MN15: A Kohn–Sham global-hybrid exchange–correlation density functional with broad accuracy for multi-reference and single-reference systems and noncovalent interactions. *Chem. Sci.* **2016**, *7*, 5032–5051.
24. Eathiraj, S.; Palma, R.; Volckova, E.; Hirschi, M.; France, D.S.; Ashwell, M.A.; Chan, T.C. Discovery of a novel mode of protein kinase inhibition characterized by the mechanism of inhibition of human mesenchymal-epithelial transition factor (c-Met) protein autophosphorylation by ARQ 197. *J. Biol. Chem.* **2011**, *286*, 20666–20676. [CrossRef] [PubMed]
25. Hu, C.; Wang, A.; Wu, H.; Qi, Z.; Li, X.; Yan, X.-E.; Chen, C.; Yu, K.; Zou, F.; Wang, W. Discovery and characterization of a novel irreversible EGFR mutants selective and potent kinase inhibitor CHMFL-EGFR-26 with a distinct binding mode. *Oncotarget* **2017**, *8*, 18359. [CrossRef]
26. Son, J.; Jang, J.; Beyett, T.S.; Eum, Y.; Haikala, H.M.; Verano, A.; Lin, M.; Hatcher, J.M.; Kwiatkowski, N.P.; Eser, P.Ö. A Novel HER2-Selective Kinase Inhibitor Is Effective in HER2 Mutant and Amplified Non–Small Cell Lung Cancer. *Cancer Res.* **2022**, *82*, 1633–1645. [CrossRef] [PubMed]
27. Subramanian, G.; Bowen, S.J.; Zhu, Y.; Roush, N.; Zachary, T.; Javens, C.; Williams, T.; Janssen, A.; Gonzales, A. Type 2 inhibitor leads of human tropomyosin receptor kinase (hTrkA). *Bioorg. Med. Chem. Lett.* **2019**, *29*, 126624. [CrossRef]
28. Roskoski Jr, R. Properties of FDA-approved small molecule protein kinase inhibitors. *Pharmacol. Res.* **2019**, *144*, 19–50. [CrossRef]
29. Sogabe, S.; Kawakita, Y.; Igaki, S.; Iwata, H.; Miki, H.; Cary, D.R.; Takagi, T.; Takagi, S.; Ohta, Y.; Ishikawa, T. Structure-based approach for the discovery of pyrrolo [3, 2-d] pyrimidine-based EGFR T790M/L858R mutant inhibitors. *ACS Med. Chem. Lett.* **2013**, *4*, 201–205. [CrossRef]
30. Dorsch, D.; Schadt, O.; Stieber, F.; Meyring, M.; Grädler, U.; Bladt, F.; Friese-Hamim, M.; Knühl, C.; Pehl, U.; Blaukat, A. Identification and optimization of pyridazinones as potent and selective c-Met kinase inhibitors. *Bioorganic Med. Chem. Lett.* **2015**, *25*, 1597–1602. [CrossRef] [PubMed]
31. Abdelaziz, A.A.S.; Nawaz, M.; Izzeldin, I.; Abubshait, H.A.; Alsadig, A.; Gomaa, M.S.; Abubshait, S.A.; Alsewdan, D. Molecular docking and Anticancer Activity of Some Synthesized 1,4- naphthoquinone Derivatives against Human Cancer Cell Line. *J. Mol. Struct.* **2023**, *1275*, 134702. [CrossRef]
32. Strzelecka, M.; Glomb, T.; Drąg-Zalesińska, M.; Kulbacka, J.; Szewczyk, A.; Saczko, J.; Kasperkiewicz-Wasilewska, P.; Rembiałkowska, N.; Wojtkowiak, K.; Jezierska, A. Synthesis, Anticancer Activity and Molecular Docking Studies of Novel N-Mannich Bases of 1, 3, 4-Oxadiazole Based on 4, 6-Dimethylpyridine Scaffold. *Int. J. Mol. Sci.* **2022**, *23*, 11173. [CrossRef]
33. Tokalı, F.S.; Taslimi, P.; Demircioğlu, İ.H.; Şendil, K.; Tuzun, B.; Gülçin, İ. Novel phenolic Mannich base derivatives: Synthesis, bioactivity, molecular docking, and ADME-Tox Studies. *J. Iran. Chem. Soc.* **2022**, *19*, 563–577. [CrossRef]
34. Demir, Y. Naphthoquinones, benzoquinones, and anthraquinones: Molecular docking, ADME and inhibition studies on human serum paraoxonase-1 associated with cardiovascular diseases. *Drug Dev. Res.* **2020**, *81*, 628–636. [CrossRef] [PubMed]

Disclaimer/Publisher's Note: The statements, opinions and data contained in all publications are solely those of the individual author(s) and contributor(s) and not of MDPI and/or the editor(s). MDPI and/or the editor(s) disclaim responsibility for any injury to people or property resulting from any ideas, methods, instructions or products referred to in the content.